https://doi.org/10.5194/amt-2020-517
Preprint. Discussion started: 16 February 2021
© Author(s) 2021. CC BY 4.0 License.

Atmospheric Measurement Techniques Discussions

Analysis of mobile monitoring data from the microAeth® MA200 for measuring changes in black carbon on the roadside in Augsburg

Xiansheng Liu[1,2], Hadiatullah Hadiatullah[3], Xun Zhang[4,5], L. Drew Hill[6], Andrew H. A. White[6,7], Jürgen Schnelle-Kreis[1], Jan Bendl[1,8], Gert Jakobi[1], Brigitte Schloter-Hai[1], Ralf Zimmermann[1,2]

[1]Joint Mass Spectrometry Center, Cooperation Group Comprehensive Molecular Analytics, Helmholtz Zentrum München, German Research Center for Environmental Health, Ingolstädter Landstr. 1, 85764 Neuherberg, Germany

[2]Joint Mass Spectrometry Center, Chair of Analytical Chemistry, University of Rostock, 18059 Rostock, Germany

[3]School of Pharmaceutical Science and Technology, Tianjin University, 300072 Tianjin, China

[4]Beijing Key Laboratory of Big Data Technology for Food Safety, School of Computer Science and Engineering, Beijing Technology and Business University, 100048 Beijing, China

[5]Key Laboratory of Resources Utilization and Environmental Remediation, Institute of Geographical Sciences and Natural Resources Research, Chinese Academy of Sciences, 100101 Beijing, China

[6]AethLabs, San Francisco, CA, USA

[7]Yale School of Medicine, New Haven, CT, USA

[8]Institute for Environment Studies, Faculty of Science, Charles University, Prague, Czech Republic

Correspondence to: Xun Zhang (zhangxun@btbu.edu.cn); Jürgen Schnelle-Kreis (juergen.schnelle@helmholtz-muenchen.de).

Abstract. The portable microAeth® MA200 (MA200) is widely applied for measuring black carbon (BC) in human exposure characterization and mobile air quality monitoring. However, the field lacks information about this instrument's performance under various settings. This study evaluated the real-time performance of the MA200 in an urban area, Augsburg, Germany. Noise reduction and negative value mitigation were explored using different data processing methods: local polynomial regression (LPR), optimized noise reduction averaging (ONA), and centered moving average (CMA) under different interval time (5s, 10s, and 30s). After noise reduction, the data were evaluated and compared by (1) the relative number of negative values; (2) more detailed microenvironmental change information retained after noise reduction; (3) the reduction of the peak values and number of peak samples; (4) more detailed microenvironmental change retained after the background correction. Our results showed that CMA showed a good prospect to analyze the raw BC concentration data in terms of the interval time due to its proportions of negative values and the detail microenvironmental change. Moreover, the CMA method has the highest reduction peak values and the number of peak samples compared to ONA and LPR. Furthermore, after background correction, the CMA treatment results remained more detailed microenvironmental changes in pollutants than others. Therefore, based on a comprehensive comparison, CMA offered a good approach to post-process the raw BC concentration

https://doi.org/10.5194/amt-2020-517
Preprint. Discussion started: 16 February 2021
© Author(s) 2021. CC BY 4.0 License.

Atmospheric Measurement Techniques Discussions

data. These findings provide new insight for the noise reduction approach that applied in mobile monitoring campaign using BC instruments.

Keywords: Black carbon; Mobile measurement; Noise reduction; Peak-value sample; Background correction

1 Introduction

Black carbon (BC) with a particle size of 0.01 to 1 μm (Zhou et al., 2020), a component of particulate matter (PM) appearing in many parts of the world, is a pollutant that encompasses a range of carbonaceous materials produced by the incomplete combustion of fossil fuel and biomass containing carbon (Goldberg, 1985). BC plays an important role in climate systems (Kutzner et al., 2018, Sadiq et al., 2015) because it is highly effective in absorbing solar radiation at visible and infrared wavelengths. However, the hyper-local nature of air quality among small-scale urban blocks is difficult to characterize with existing fixed monitoring stations (Apte et al., 2017), especially for on-road concentrations. Therefore, the field needs a reasonable and effective way to study differences in urban air quality on a small (micro) scale, to explore the causes of hyper-local differences in air quality, and to propose monitoring methods on air pollution situation in urban cities.

A new instrument, the microAeth® MA200 (MA200; AethLabs, San Francisco, CA, USA) was recently developed for measuring personal exposures to BC, ambient and vertical profiles of BC, and emissions of BC from indoor sources, among other BC phenomena. The MA200 continuously collects aerosol particles on a filter and measures the optical absorption at 5 wavelengths (880, 625, 528, 470, and 375 nm) with a data collection time-base as frequent as 1Hz. The cross-spectrum measurement provides insight into the composition of light-absorbing carbonaceous particles and helps to distinguish among the different optical signatures of various combustion sources such as fossil fuel (e.g., diesel) and biomass and tobacco combustion. The instruments support the DualSpot® loading compensation method, which corrects for the optical loading effect (Virkkula et al., 2007) and provides additional information about aerosol optical properties. In our study, the equivalent black carbon, eBC, was used when addressing quantitative values.

Generally, negative values may appear if the measurement is applied in an environment with low BC concentration or high time resolution. This is due to the use of an incremental optical attenuation value (ATN) to calculate the BC value. Even negative values usually contain valid information that is required for noise reduction or smoothing the data over a longer time interval, simply removing negative values may therefore be harmful to the dataset. Therefore, noise reduction of the raw data is highly recommended to enhance the data quality without losing temporal resolution accuracy (Liu et al., 2020a). Moreover, the measurement of time-averaged roadside air quality, for example, passing vehicles, may bias estimates of typical local concentrations due to their contribution of peak-value measurements to the dataset. Meanwhile, when sampling equipment enters from a highly polluted environment to lower polluted surroundings, such as a park, the original concentration will produce

https://doi.org/10.5194/amt-2020-517
Preprint. Discussion started: 16 February 2021
© Author(s) 2021. CC BY 4.0 License.

Atmospheric Measurement Techniques Discussions

negative peak noise due to the complex environment of the sampling site. Therefore, the noise reduction method should be optimized to obtain the actual peak concentration and peak samples, which facilitates for identifying the source of pollution.

In addition, air pollution concentrations at a specific time and place can be comprised of two primary aspects, including contributions from local source emissions and a background concentration. Background concentration, especially the high background concentration of typical pollution events (such as haze), tends to obscure or even conceal the contribution of local sources of pollution (Van Poppel et al., 2013). Moreover, the real-time changes in local sources, meteorology, and regional transport will cause changes in the pollution background (Brantley et al., 2014), which will affect the comparability of measurements between different days or even at different times on the same days. Due to this phenomenon, the noises were frequently found in mobile monitoring data. Therefore, the optimization of noise reduction data was required by the correction of background concentration,which provided a better analysis to the contribution of local pollution sources.

This study evaluated methods for noise reduction mobile measurement data of roadside by BC in an urban area by using optimized noise reduction averaging (ONA) algorithm, local polynomial regression (LPR), and centered moving average (CMA). Further evaluations, based on (1) the relative number of negative values; (2) detailed microenvironmental change information (3) the peak values reduction; (4) detailed microenvironmental change after the background correction, were analyzed to select the best noise reduction approach.

2 Methods

2.1 Instrumentation

In this study, personal exposure monitors for BC (microAeth® MA200; AethLabs, San Francisco, CA, USA) were used simultaneously to measure BC levels at the city center. The MA200 senses 5 optical wavelengths per measurement: infrared, red, green, blue, and ultra-violet (880, 625, 528, 470, and 375 nm, respectively). The detection limit is 30 ng/m^3 and the measurement resolution 1 ng/m^3 (aethlabs.com). In mobile monitoring, the MA200 can be used to estimate exposure and quantify environmental concentrations. It can help to identify hot spots and to quantify BC levels on roads and highways as well as in various other mobile environments (Apte et al., 2011, Dons et al., 2012, Madueño et al., 2019) including bicycles (Wójcik et al., 2014, Samad and Vogt, 2020), trains (Andersen et al., 2019), and airplanes (Kim et al., 2019). The device can also be applied in long-term stationary monitoring, vertical profiling, and atmospheric measurement with unmanned aerial vehicles (Cao et al., 2020, Chiliński et al., 2018, Pikridas et al., 2019), balloons (Ferrero et al., 2016, 2014, 2011, Markowicz et al., 2017, Samad and Vogt, 2020), community monitoring, indoor air quality monitoring, and the assessment of personal exposure and related health effects (Isley et al., 2017). In order to reduce the noise of data obtained with high time resolution, the data measured by the instrument can be smoothed.

https://doi.org/10.5194/amt-2020-517
Preprint. Discussion started: 16 February 2021
© Author(s) 2021. CC BY 4.0 License.

Atmospheric Measurement Techniques Discussions

AethLabs offers tools for applying several noise reduction algorithms to MA-series and AE51 device data on its website (https://aethlabs.com [note: a free account is required]). To evaluate the relative performance of MA200, this study was analyzed BC data collected from multiple MA200 devices, identified individually by serial numbers (MA200-0051, MA200-0053, MA200-0059, MA200-0060, MA200-0155, MA200-0153, MA200-159) and used the MA200's onboard signal-processing to moderately reduce the noise of the BC signal. Comparative measurements of the microAeth® MA200 and a stationary Aethalometer (AE33, Magee Scientific, Berkeley, USA) showed good agreement of stationary measurements carried out between the individual walks (Liu et al., 2020b). Information about the date, duration, and time resolution (time base) of each MA200 device as used during measurement for this study are summarized in Table 1. To give intercomparison between the instruments, and also to demonstrate whether they are giving consistent measurements across different instruments, we performed the comparative measurements test for the different MA200 in fixed monitoring stations and mobile monitoring road (Table S1 and Fig. S1). The results showed that there were no significant wavelength dependence between different instruments.

Table 1 Measurements of black carbon by different MA200 devices.

Measurement number	Date (dd/mm/yyyy)	Serial number	Start time (hh:mm:ss)	End time (hh:mm:ss)	Time base (s)	Site
1	27/09/2018	MA200-0051	10:29:10	13:38:20	10	Augsburg, Germany
2	15/11/2018	MA200-0059	11:53:42	16:13:12	10	
3	16/11/2018	MA200-0053	11:34:06	16:33:56	10	
4	26/08/2019	MA200-0060	11:01:56	15:44:46	10	
5	21/02/2020	MA200-0155	10:00:10	13:10:00	5	
6	21/02/2020	MA200-0153	10:00:10	13:10:00	10	
7	21/02/2020	MA200-0159	10:00:10	13:10:00	30	
8	24/11/2020	MA200-0059	09:40:57	11:09:07	10	Munich, Germany
9	01/12/2020	MA200-0051	13:29:05	15:19:00	5	
10	18/12/2020	MA200-0051	14:39:30	15:19:30	30	

2.2 Study design and route

The MA200 instrument is able to measure in 1 s, 5 s, 10 s, 30 s, 60 s, and 300 s time intervals. The 1 s time base exhibits the most challenging interpretation because of poor signal to noise ratio especially at low concentrations, as is similar to other optical black carbon monitors (Hagler et al., 2011). 1 s measurement resolution therefore may be most useful when sampling in high concentration environments, performing direct emissions testing, or for applications that require high time resolution. However, the BC average concentration is not high enough for this analysis in the city center of Augsburg, Germany, (measured at 2.62 μg/m^3 in winter by Gu, (2012)) thus we did not use the 1 s time base. Moreover, 60 s and 300 s for mobile monitoring are too long which will affect the accuracy of the spatial variation of pollutants, hence both time bases were not selected in this study. In order to better understand at which time interval sampling might be most useful in this context, mobile measurements

https://doi.org/10.5194/amt-2020-517
Preprint. Discussion started: 16 February 2021
© Author(s) 2021. CC BY 4.0 License.

Atmospheric Measurement Techniques Discussions

at low BC concentrations, three MA200 devices were used in parallel to measure black carbon concentrations with the time intervals of 5 s, 10 s, and 30 s (Measurement numbers 5-7 in Table 1).

To control for relative patterns in environmental exposures, a fixed walking path within the center of the city was determined. Wherever possible, the routes were carried out on the right side of the road due to people's daily habits (driving and walking on the right side in Germany). All walks along the route were conducted on weekdays, with clear skies and calm winds to avoid misrepresentation of typical urban air exposure conditions. The route started from Augsburg University of Applied Sciences and continued approximately 14 km for 4 h with average walking time, passing through different types of land use to ensure that different microenvironments were represented and to generalize the validity of the results in the different urban areas. Briefly, the study was composed of the following phases, (1) collecting raw BC data using the sampling instruments (MA200); (2) smoothing the acquired raw BC data under different noise reduction methods; (3) comparing the noise reduction data based on the detail change of value characters and number of negative value; (4) following the peak values identification by COV approach and (5) following the background estimation and correction by TPRS approach; (6) finally, selecting the best noise reduction approach.

2.3 Instrumentation preparation

Instrument preparation took place in our laboratory before each walk and consisted of “zero” calibration checks, the examination of the MA200 filter cassette, battery, GPS, and memory checks. Flow calibrations were performed with a factory-calibrated flow meter (Alicat Scientific, Inc. Tucson, AZ, USA).

2.4 Noise reduction methods

2.4.1 ONA (optimized noise-reduction averaging)

The principle of the ONA is based on the time series of three parameters in the original observation data, namely the observation time, the original BC concentration, and the optical attenuation (ATN), as specifically described in Hagler et al. (2011). When the ONA method is used, the incremental light attenuation (ΔATN) needs to be determined. Hagler et al., (2011) showed that the black carbon data obtained by the instrument (various Aethalometer models, AE21, AE42, and AE51) at the fixed monitoring site, in the data post-processing, used ΔATN= 0.05. However, when the ΔATN=0.05 is applied by MA200, the black carbon noise reduction data is too smooth, hence, ΔATN=0.01 was selected to capture more details of the variability (Figure S2).

2.4.2 LPR (local polynomial regression)

LPR is a useful non-parametric regression tool to explore fine data structures and has been widely used in practice. LPR is similar to a moving average but employs polynomial regression rather than simple averaging (Masry, 1996, Breidt and Opsomer, 2000). Choosing the Smoothing number of points is necessary before LPR. The smoothing should be chosen to balance effective smoothing of the

https://doi.org/10.5194/amt-2020-517
Preprint. Discussion started: 16 February 2021
© Author(s) 2021. CC BY 4.0 License.

Atmospheric Measurement Techniques Discussions

measured values and spatial resolution (distance). The distance resolution was chosen at approximately about 100 m. Supposing the sampling speed is 1.5 m/s, when the interval time is 5 s, 10 s, and 30 s, the number of smoothing data points are 15, 7, and 3, respectively.

2.4.3. CMA (centered moving average)

The centered moving average is a smoothing technique that is used to make the long term trends of a time series clearer (Easton and McColl, 1997). There is no shift or group delay in the data using the centered moving average, unlike a simple moving average. The centered moving average can only be applied in noise reduction as it requires data from both before and after each smoothed data point. To determine the number of data points to be averaged, the criteria discussed above for LPR apply.

2.5 Comparison analysis after noise reduction approach

2.5.1 The detailed effect of microenvironmental change information

After the noise reduction, the number of negative values was calculated for selecting the best method. Meanwhile, according to the change graph of the noise reduction data, the microenvironmental change information was analyzed and compared as another factor for selecting the best method. If the microenvironmental change information remains more detailed, it implies that the method can reflect the subtle changes in the microenvironmental pollutants, which is favorable to identify the pollution sources. However, if the microenvironmental change information is less detailed, the pollution source may be hard to be identified. Therefore, more detailed change information can be selected as the best option to provide accurate information.

2.5.2 Peak-value sample identification

A recent paper by Brantley et al (2014) compared several methods for detecting and eliminating peak-value samples in mobile air pollution measurements. These include identifying samples outside of a threshold based on a median produced using road segmentation, an α-trimmed arithmetic average (Van den Bossche et al., 2015), a running coefficient of variation (COV) (Hagler et al., 2012), an estimate of background standard deviation (Drewnick et al., 2012), a running low 25 % quantile (Choi et al., 2012) and 3 times the standard deviation (Wang et al., 2015). The formula for the running method used in this analysis is previously described by Hagler et al. (2012) with minor modification (Eq. 1):

$$COV_t = \frac{\sqrt{\frac{1}{7}\sum_{i=t-3}^{i=t+3}(x_i - \bar{x})^2}}{\bar{x}_{all}} \quad (1)$$

Where COV_t is the 70 s sliding coefficient of variation of the t-th BC sample, x_i is the i-th BC sample, $\bar{x}$ is the average of the t-th BC sample and the three samples before and after it, and $\bar{x}_{all}$ is the average of all BC samples in one experiment. The 99th quantile of the 70 s sliding coefficient of variation of all

https://doi.org/10.5194/amt-2020-517
Preprint. Discussion started: 16 February 2021
© Author(s) 2021. CC BY 4.0 License.

Atmospheric Measurement Techniques Discussions

BC samples is used as the threshold for determining "peak-value". The BC samples that are greater than this threshold are flagged as peak-value samples along with the BC samples 3 data points before and after.

2.5.3 Background estimation and correction

Background correction methods include the single sample standardization method, the sliding minimum method, the linear regression smoothing method, and the spline (of minimum) regression smoothing method. Brantley et al. (2014) suggested that a thin plate regression spline (TPRS) method can reliably evaluate the background value of mobile measurements, and, thus, is the method chosen for this analysis to compare the data obtained after the noise reduction approach. Briefly, the TPRS approach includes three steps: (1) Process the noise reduction data of pollutant sample with a 30 s moving average; (2) sequentially process the results of the 30 s moving average by the specified time window (e.g. 10 min) and identify the position of the minimum sample of pollutant concentration in each aliquot window; (3) use thin-plate spline regression to smoothly fit the sample of minimum pollutant concentration obtained in step (2).

Following the above analysis, the criteria to select the noise reduction methods based on (1) the relative number of negative values; (2) more detailed microenvironmental change information retained after noise reduction; (3) the reduction of the peak values and number of peak samples; (4) more detailed microenvironmental change retained after the background correction.

3 Results and discussion

3.1 Noise reduction data under different interval time

As shown in Figure 1, three MA200s were used at the time bases of 5 s, 10 s, and 30 s. The proportions of negative values in raw data were 42.1 %, 37.6 %, and 30.5 %, respectively (Fig. 1a, Table 2). The experimental data at each time interval were processed by the smoothing methods ONA, LPR, and CMA (Figs. 1b, 1c and 1d).

In the 5 s time base data, the BC values changed very rapidly, and the ONA method could not be used (Fig. 1b). For this dataset, only one value remained negative after smoothing. We found that when the time interval is 5 s, all ΔATN ($ATN_{t(0)+\Delta t'}-ATN_0$) data are negative in the raw data, which causes the negative value of black carbon after the ONA method (Hagler et al., 2011). After smoothing, negative values retained 33.3 % for LPR and 26.1 % for CMA. In the 10 s interval cohort for peak-values, there were no negative values after ONA processing, suggesting that a strong smoothing effect is obtained at low-values. After smoothing, negative values retained 30.2 % for LPR and 25.3 % for CMA. In the 30 s interval data, after smoothing, the negative values comprised 0 % for ONA, 25.5 % for LPR, and 22.4 % for CMA. The 30 s interval dataset presented the lowest proportion of negative values both before and after application of the three smoothing treatments, likely due to the longer intervals of sampling which also imbued each datapoint with a large spatial rang. The mobile monitor covers

https://doi.org/10.5194/amt-2020-517
Preprint. Discussion started: 16 February 2021
© Author(s) 2021. CC BY 4.0 License.

Atmospheric Measurement Techniques Discussions

longer distances over longer measurement periods. Thus, when the monitoring instrument runs for 30 s, hot spots are more difficult to identify.

The ONA method shows significant effects on the smoothing of negative values (Fig. 1b). However, the ONA-processed data are so smooth that they may omit micro-environmental changes information. For example, Figure 2, interval time 10 s. LPR and CMA smoothing, however, are capable of mitigating negative values while retaining many of the original data characteristics, potentially allowing researchers to analyze the temporal and spatial changes in pollutant concentrations with more sensitivity to local events and sources.

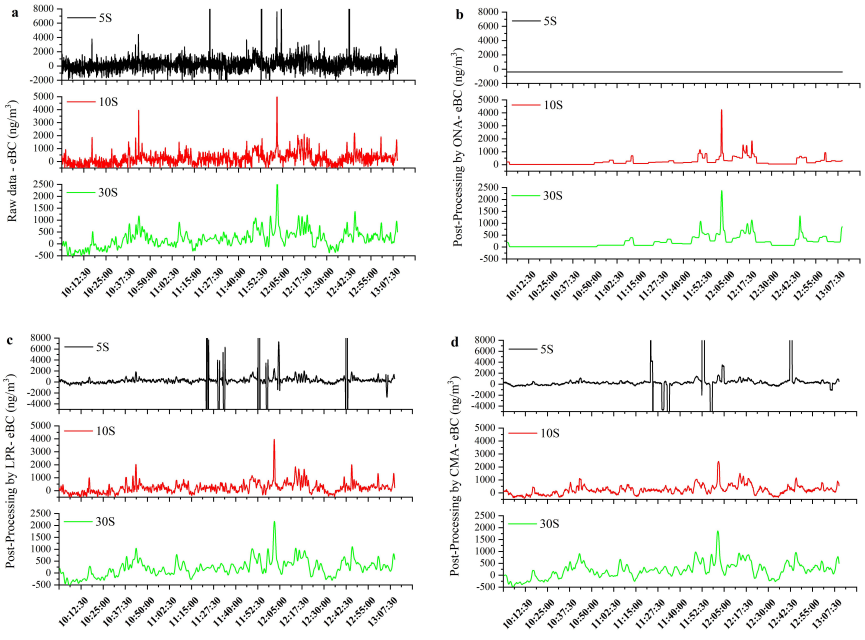

Figure 1 The temporal fluctuations of the BC levels measured with the MA200 at sampling time bases of 5 s, 10 s, and 30 s during a typical sampling period (about 190 min) **(a)**, raw data without noise reduction, **(b)**, data treated with ONA, **(c)**, data treated with LPR, and **(d)**, data treated with CMA. The analysis based on data from measurements 5, 6, and 7, that were one run with three MA200 measuring parallel.

https://doi.org/10.5194/amt-2020-517
Preprint. Discussion started: 16 February 2021
© Author(s) 2021. CC BY 4.0 License.

Atmospheric Measurement Techniques Discussions

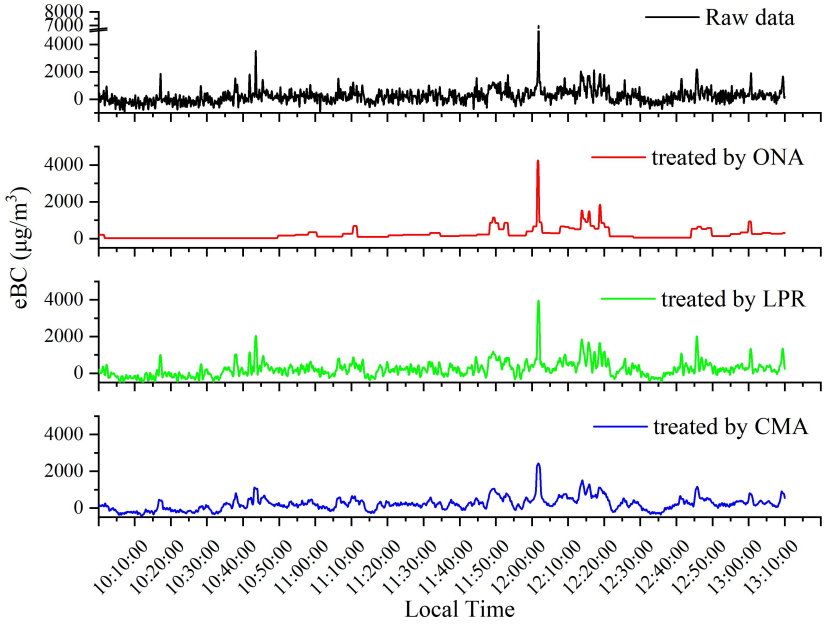

Figure 2 The temporal fluctuations of the BC levels measured with the MA200 at sampling time base10 s based on the three methods (the analysis based on measurement 6).

Table 2 The proportion of negative values in original runs and each run under the different smoothing methods (values are shown as (%), -, no data).

Interval time	Factor	RAW	ONA	LPR	CMA	Negative decline rate
5 s	Negative values	42.06	-	33.33	26.14	37.85
	Noise reduction effect	100	-	37.53-72.61	57.05-96.56	-
10 s	Negative values	37.63	0	30.23	25.26	32.87
	Noise reduction effect	100	51.37-78.64	53.24-68.95	71.93-81.14	
30 s	Negative values	30.53	0	25.53	22.37	26.73
	Noise reduction effect	100	24.65-82.24	45.70-52.32	47.04-67.29	

3.2 Comparison of peak samples after noise reduction methods

The processing of peak sample is an important evaluation index for the measurement of time-averaged roadside air quality, for example, passing vehicles may bias estimates of typical local concentrations due to their contribution of peak-value measurements to the dataset. Therefore, after noise reduction, we compare the reduction values and the number of peak samples to further evaluate the noise reduction methods.

https://doi.org/10.5194/amt-2020-517
Preprint. Discussion started: 16 February 2021
© Author(s) 2021. CC BY 4.0 License.

Atmospheric Measurement Techniques Discussions

For reduction of peak-values, in the interval time 5 s, the average reduction effect of the LPR and CMA methods are 58.82 % and 82.23 %, respectively, (ONA method cannot be used). In the interval time 10 s, the average reduction effect of the CMA processing (77.77 %) is higher than that of both ONA (65.00 %) and LPR (61.83 %). In the interval time 30 s, after ONA, LPR, and CMA processing, CMA presented the greatest average of peak-value reduction effect (58.09 %), while ONA (41.67 %) and LPR (48.99 %) presented the average peak-value reduction effects. Taken together, CMA has the greatest reduction of peak-value (Table 2).

For the number of peak samples, after noise reduction, the peak value samples were identified by the COV method accounted of 36 % for ONA, 47 % for LPR, and 60 % for CMA based on the number of each run, suggesting that the CMA method has the highest reduction of the peak values number (Table S2). Hence, it worth noting that CMA is indirectly performed well to facilitate appropriate data after noise reduction based on the reduced number of peak values.

Even though the peak values can affect the average of the pollutants concentration, however, from the perspective of exposure characteristics, they are still included as actual exposures and provide valuable information for mobile measurements, such as identification of the pollution source. In addition, to further characterize the distribution of the peak values concentration, therefore, we select one of run after CMA (Measurement 6) for analysis (Fig. 3). As shown in Figure 3, eBC values along the main roads and at intersections were higher than at other locations, presumably due to a large part of stop-and-go for traffic or cars in front of or around the mobile monitor (Figs. 3a and b). It can be seen from Figures 3a and b that the peak-values of BC samples were mainly found in 4 locations, represented by red triangles (Fig. 3a). The vehicles are frequently found in these locations that may relatively affect the increased or decreased road traffic depending on the time of measurement. The highest eBC values were repeatedly found in streets with fairly high traffic volumes and dense coverage with relatively tall buildings (street canyon situation). Therefore, the change of air pollution in urban micro-environments is the combined effects of traffic and location (Buonanno et al., 2011). In short, after CMA treatment, the peak value and the number of peak samples are greatly reduced, which is helpful to identify the actual peak sample location and further identify the source of pollution.

https://doi.org/10.5194/amt-2020-517
Preprint. Discussion started: 16 February 2021
© Author(s) 2021. CC BY 4.0 License.

Atmospheric Measurement Techniques Discussions

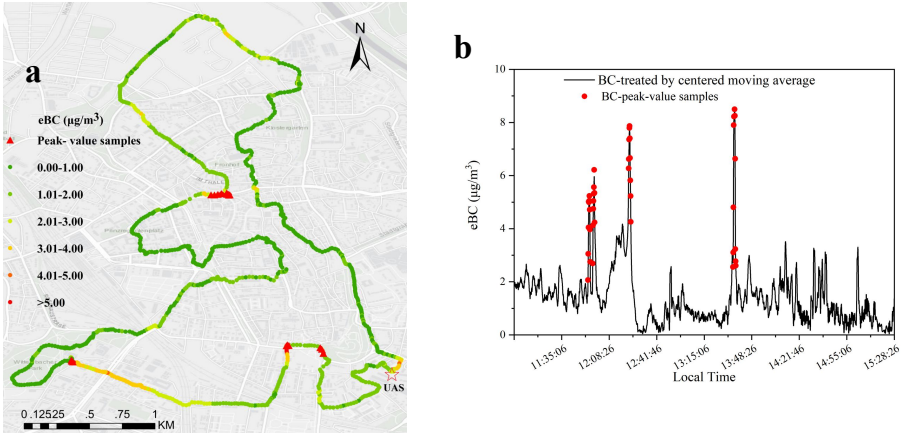

Figure 3 Identification of the spatial **(a)** and temporal **(b)** distribution characteristics of BC peak-value samples based on the COV method (the analysis based on measurement 6), © OpenStreetMap contributors. Distributed under a Creative Commons BY-SA License.

3.3 Comparison of background estimation and correction after noise reduction methods

Adopting a reasonable background correction method to remove the background contribution in pollution observations and highlight the contribution of local pollution sources is conducive to the effective formulation of urban local emission reduction strategies. Because of the real-time changes in citywide sources of pollution, the transportation of regional pollution and meteorological conditions will lead to changes in the background concentration, which in turn affects the comparability of pollution observation results within a day or between different days (Brantley et al., 2014). However, after different noise reduction approaches, the background correction concentration is different, therefore, further evaluation on their background correction concentration was necessary for this study.

After noise reduction methods, the data was evaluated using the TPRS method, we calculated the 5 min and 10 min background concentrations under different noise reduction approaches. As shown in Figure 4a and b, after comparing the background concentration under different noise reduction approaches, the background concentration after LPR has the largest negative number proportion and minus absolute value, affecting the greater of the background-corrected concentration than the actual monitoring concentration. However, the background concentrations after ONA and CMA show a few numbers of negative proportion and minus absolute value. Therefore, to further compare the ONA and CMA approach, we compared the concentration characteristic after background correction (Figs. 4c and d). As shown in Figures 4c and d, when the concentration is lower than 1 μg/m^3, the background correction results after ONA treatment are smoother, which hardly reflects more detailed microenvironmental changes in pollutants.

https://doi.org/10.5194/amt-2020-517
Preprint. Discussion started: 16 February 2021
© Author(s) 2021. CC BY 4.0 License.

Atmospheric Measurement Techniques Discussions

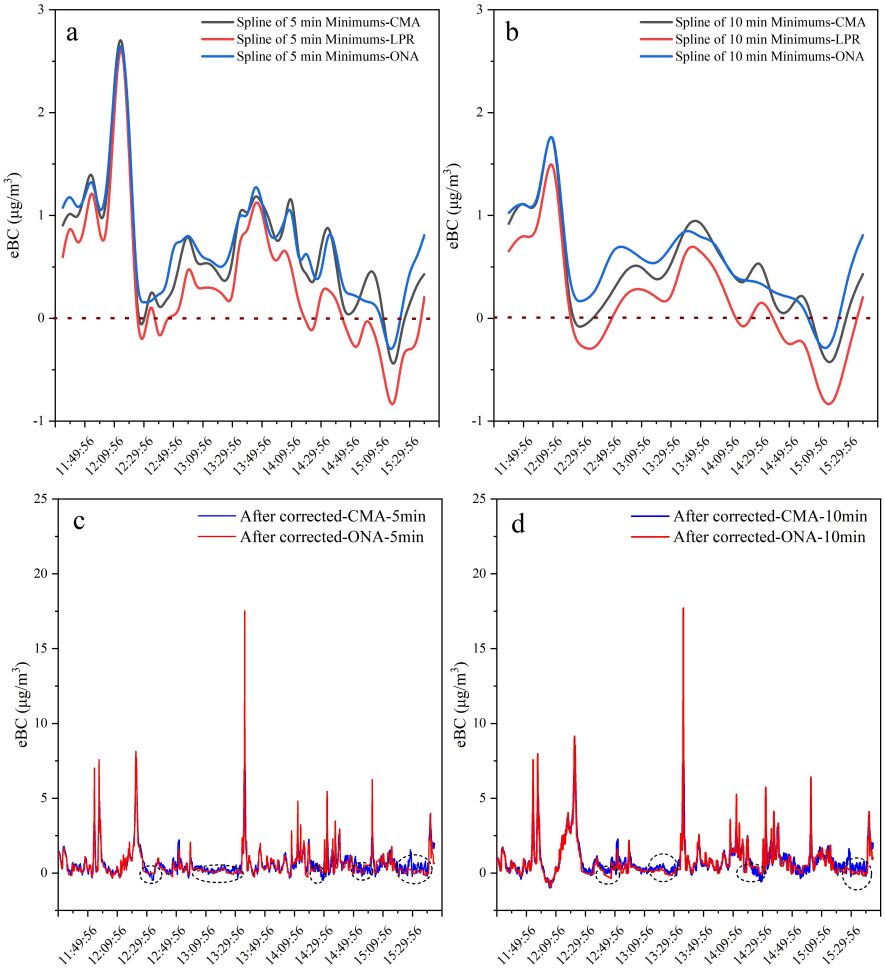

315 **Figure 4** Time-series methods: **(a)**, spline of 5 min minimums, (b), spline of 10 min minimums under different noise reduction methods, **(c)**, the background concentration and actual detection concentration after CMA and, **(d)**, ONA (the analysis based on the measurement 4).

In order to certify the CMA applicability and its advantages of the background correction method, this study further analyzed the BC concentrations measured by a fixed background monitoring station in 320 Augsburg, located in the urban background on the campus of the University of Applied Sciences (UAS) (Cyrys et al., 2006) (Fig. S3). The background value under the 5 minutes ("min") window exhibits undulating characteristics, and the fitting curve in the 10 min window is relatively smooth. However, the TPRS-based background value often does not fluctuate greatly over short periods, and the BC background value curve under the 5 min window does not conform to the "actual" urban background 325 situation as estimated using data from the fixed-site monitor. Moreover, by comparing the curve produced by the spline of 10 min minimums with the BC background concentration as measured by the

https://doi.org/10.5194/amt-2020-517
Preprint. Discussion started: 16 February 2021
© Author(s) 2021. CC BY 4.0 License.

Atmospheric Measurement Techniques Discussions

fixed monitoring station (Background-UAS, Figure S3), it can be found that the background correction method based on the time series can well characterize the time-varying characteristics of the polluted background in each experiment, suggesting that, of the two options, 10 min showed the better window for fitting the background value curve of BC.

Under the TPRS method, the background concentration of BC can be fitted at each moment of sampling. The TPRS-estimated background contribution of the observed BC concentration averaged 37.8 % of the total measured concentration. However, when examining the contribution of background concentration of pollutants in a single measurement, a large fluctuation (10.4 -71.3 %) is noted, which may be closely related to sizeable changes in the meteorological conditions, traffic conditions along the road (and overtime at the same point in the road), and urban street canyon effects in each test. Therefore, based on the comparison of background correction, the CMA results showed better applications for estimating the background concentration and location source contribution.

3.4 Generalization of the treatment

To verify the generalization ability of this approach, we performed another three sampling routes in Munich (Measurement 8, 9, 10). After obtained the raw data, the noise reduction data were performed by CMA (Fig. S4). The results showed that the following methods have the ability for application in a different location and are widely used in other environments as compared with the original route (Augsburg). In this comprehensive comparison of MA200 BC data, the CMA processing method showed the greatest potential to smooth out negative values while maintaining spatial and temporal nuances in our measurement environment across each of the time bases examined (5 s, 10 s, and 30 s). Therefore, based on the above analysis, the summary of the decision tree was proposed in this study (Scheme 1).

https://doi.org/10.5194/amt-2020-517
Preprint. Discussion started: 16 February 2021
© Author(s) 2021. CC BY 4.0 License.

Atmospheric Measurement Techniques Discussions

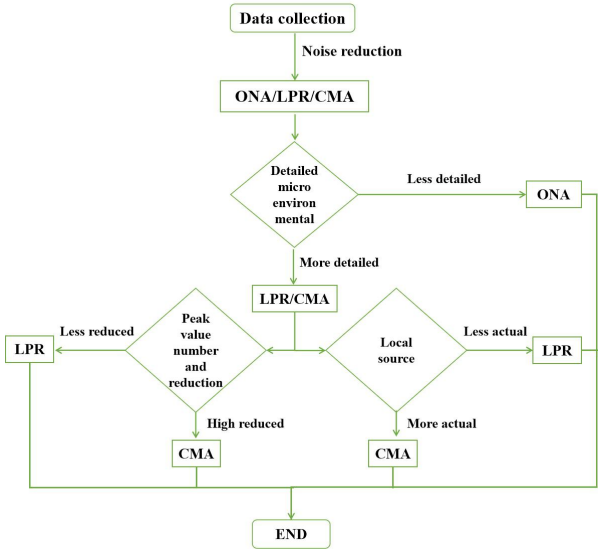

Scheme 1 The proposed decision tree for mobile monitoring data from the microAeth® MA200.

4 Conclusion

The black carbon monitoring equipment, microAeth® MA200, was used in the city center of Augsburg, Germany to assess BC pollution along a predetermined route, exploring different micro-environments as well as different sampling time intervals. Our results showed that, in terms of the interval time of 5 s, 10 s, and 30 s, after smoothing, CMA showed good prospect to analyze the raw BC concentration data based on the detailed microenvironmental characteristic, and proportions of negative values. The further evaluation by peak-value reduction effects and the peak values number, the CMA method has the highest reduction compare to ONA and LPR, suggesting that CMA performed well to facilitate an appropriate data after noise reduction approach. Following background estimation and correction, the background concentrations after ONA and CMA show a few numbers of negative proportion and minus absolute value. However, after CMA treatment, the background correction results reflect more detailed microenvironmental characteristics in pollutants. Therefore, based on the comprehensive comparison, the centered moving average (CMA) performed a good approach to post-process the raw BC concentration data. Further analysis is needed to understand how well these findings, which are valid for the context of our study, can apply in other contexts, such as different seasons and diurnal time.

Data availability

The all data is available on request by contacting the first author of the paper.

https://doi.org/10.5194/amt-2020-517
Preprint. Discussion started: 16 February 2021
© Author(s) 2021. CC BY 4.0 License.

Atmospheric Measurement Techniques Discussions

370 **Author contribution**

Data curation, X.L; Funding acquisition, X.Z.; Investigation, J.SK, G.J and R.Z; Methodology, X.L. and H.H; Project administration, X.Z.; Software, X.L.; Supervision, J.SK.; Visualization, J.B; Writing-original draft, X.L.; Writing-review & editing, L. DH, A. W, and B. SH.

Competing Interest

375 The authors declare that they have no conflict on interests.

Acknowledgement

We gratefully thank Erik Hopp (AethLabs, San Francisco, CA, USA) for the implementation and maintenance of the AethLabs data processing web tool.

Financial support

380 The work is funded by the Germany Federal Ministry of Transport and Digital Infrastructure (BMVI) as part of SmartAQnet (grant No.19F2003B), and by the Research Project of Ministry of Science and Technology of China (2019YFC0507800) and Support Project of High-level Teachers in Beijing Municipal Universities in the Period of 13th Five - year Plan (CIT&TCD201904037).

References

385 Andersen, M. H. G., Johannesson, S., Fonseca, A. S., Clausen, P. A., Saber, A. T., Roursgaard, M., Loeschner, K., Koponen, I.K., Loft, S., Vogel, U., and Møller P.: Exposure to air pollution inside electric and diesel-powered passenger trains, Environ. Sci. Technol., 53, 4579-4587, https://doi.org/10.1021/acs.est.8b06980, 2019.

Apte, J. S., Kirchstetter, T. W., Reich, A. H., Deshpande, S. J., Kaushik, G. C. A., Marshall, J, D., and
390 Nazaroff, W. W.: Concentrations of fine, ultrafine, and black carbon particles in auto-rickshaws in New Delhi, India, Atmos. Environ, 45, 4470-4480, https://doi.org/10.1016/j.atmosenv.2011.05.028, 2011

Apte, J. S., Messier, K. P., Gani, S., Brauer, M., Kirchstetter, T. W., Lunden, M. M., Maeshall, J. D., Portier, C. J., Vermeulen, R. C. H., and Hameurg, S. P.: High-Resolution Air Pollution Mapping with Google Street View Cars. Exploiting Big Data, Environ. Sci. Technol., 12, 6999-7008,
395 https://doi.org/10.1021/acs.est.7b00891, 2017.

Brantley, H., Hagler, G., Kimbrough, S., Williams, R., Mukerjee, S., and Neas, L.: Mobile air monitoring data-processing strategies and effects on spatial air pollution trends, Atmos. Meas. Tech., 7, 2169-2183, https://doi.org/10.5194/amt-7-2169-2014, 2014

Breidt, F. J. and Opsomer. J. D.: Local polynomial regression estimators in survey sampling. Annals of
400 Statistics 28, 1026-1053, https://www.jstor.org/stable/2673953, 2000.

Buonanno, G., Fuoco, F. C., and Stabile, L.: Influential parameters on particle exposure of pedestrians

https://doi.org/10.5194/amt-2020-517
Preprint. Discussion started: 16 February 2021
© Author(s) 2021. CC BY 4.0 License.

in urban microenvironments, Atmos. Environ, 7, 1434-1443, https://doi.org/10.1016/j.atmosenv.2010.12.015, 2011

Cao, R., Li, B., Wang, H. W., Tao, S., Peng, Z. R., and He, H. D.: Vertical and Horizontal Profiles of Particulate Matter and Black Carbon Near Elevated Highways Based on Unmanned Aerial Vehicle Monitoring, Sustainability 12, 1204, https://doi.org/10.3390/su12031204, 2020.

Chiliński, M. T., Markowick, K. M., and Kubicki, M.: UAS as a Support for Atmospheric Aerosols Research: Case Study, Pure Appl. Geophys., 9, 3325-3342, https://doi.org/10.1007/s00024-018-1767-3, 2018.

Choi, W., He, M., Barbesant, V., Kozawa, K. H., Mara, S., WIiner, A. M. Paulosn, and S. E.: Prevalence of wide area impacts downwind of freeways under pre-sunrise stable atmospheric conditions, Atmos. Environ, 62, 318-327, https://doi.org/10.1016/j.atmosenv.2012.07.084, 2012.

Cyrys, J., Pitz, M., Soentgen, J., Zimmermann, R., Wichmann, H. E., and Peters, A.: New Measurement Site for Physical and Chemical Particle Characterization in Augsburg. Germany, Epidemiology (Cambridge, Mass.) 17, S250-S251, 2006.

Dons, E., Int Panis, L., Van Poppel, M., Theunis, J., and Wets, G.. Personal exposure to Black Carbon in transport microenvironments, Atmos. Environ, 55, 392-398, https://doi.org/10.1016/j.atmosenv.2012.03.020, 2012

Drewnick, F., Böttger, T., Von Der Weiden-Reinmüller, S. L., Zorn, S. R., Klimach, T., Schneider, J., and Borrmann, S.: Design of a mobile aerosol research laboratory and data processing tools for effective stationary and mobile field measurements, Atmos. Meas. Tech, 5(6), 1443-1457, https://doi.org/10.5194/amtd-5-2273-2012, 2012.

Easton, V. J., and McColl, J. H.: Statistics Glossary v1.1, 1997.

Ferrero, L., Caooelletti, D., Busetto, M., Mazzola, M., Lupi, A., Lanconelli, C., Becagli, S., Traversi, R., Cauazzo, L., Giardi, F., Moroin, B., Crocchianti, S., Fierz, M., Močnik, G., Sangiorgi, G., Perrone, M. G., Maturilli, M., Vitale, V., Udisti, R., and Bolzacchini, E.: Vertical profiles of aerosol and black carbon in the Arctic: a seasonal phenomenology along 2 years (2011–2012) of field campaigns, Atmos. Chem. Phys, 16, 12601-12629, https://doi.org/10.5194/acp-16-12601-2016, 2016

Ferrero, L., Castelli, M., Ferrini, B. S., Moscatelli, M., Perrone, M. G., Sangiorgi, G., Rovelli, G., D'Angelo, L., Moroni, B., Scardazza, F., Mocnik, G., Bolzacchini, E., Petitta, M., and Cappelletti, D.: Impact of black carbon aerosol over Italian basin valleys: High-resolution measurements along vertical profiles, radiative forcing and heating rate, Atmos. Chem. Phys, 18, 9641 – 9664, http://dx.doi.org/10.5194/acp-14-9641-2014, 2014.

Ferrero, L., Mocnik, G., Ferrini, B. S., Perrone, M., Sangiorgi, G., and Bolzacchini, E.: Vertical profiles of aerosol absorption coefficient from micro-Aethalometer data and Mie calculation over Milan, Sci. Total Environ., 409, 2824-2837, https://doi.org/10.1016/j.scitotenv.2011.04.022, 2011.

Goldberg, E. D.: Black carbon in the environment: properties and distribution, Environ. Sci. Technol., 172-187, 1985.

Gu, J., 2012. Characterizations and sources of ambient particles in Augsburg. Germany.

Hagler, G. S. W., Lin, M., Khlystov, A., Baldauf, R. W., Isakov, V., Faircloth, J., and Jackson, L. E.: Field investigation of roadside vegetative and structural barrier impact on near-road ultrafine particle

https://doi.org/10.5194/amt-2020-517
Preprint. Discussion started: 16 February 2021
© Author(s) 2021. CC BY 4.0 License.

concentrations under a variety of wind conditions, Sci. Total Environ., 416, 7-15, https://doi.org/10.1016/j.scitotenv.2011.12.002, 2012

Hagler, G.S., Yelverton, T.L., Vedantham, R., Hansen, A.D. and Turner, J.R.: Post-processing Method to Reduce Noise while Preserving High Time Resolution in Aethalometer Real-time Black Carbon Data, Aerosol Air Qual. Res. 11: 539-546. https://doi.org/10.4209/aaqr.2011.05.0055, 2011.

Isley, C. F., Nelson, P. F., Taylor, M. P., Mani, F. S., Maata, M., Atanacio, A., Stelcer, E., and Cohen, D. D.: PM2.5 and aerosol black carbon in Suva, Fiji, Atmos. Environ, 150, 55-66, https://doi.org/10.1016/j.atmosenv.2016.11.041, 2017.

Kim, C., Kim, K. J., and Lee, J.: Assessment of black carbon concentration as a potential measure of air quality at multi-purpose facilities, J. Aerosol Sci, 138, 105450, https://doi.org/10.1016/j.jaerosci.2019.105450, 2019.

Kutzner, R. D., von Schneidemesser, E., Kuik, F., Queddenau, J., Weatherhead, E. C., and Schamle, J.: Long-term monitoring of black carbon across Germany, Atmos. Environ, 185, 41-52, https://doi.org/10.1016/j.atmosenv.2018.04.039, 2018.

Liu, X., Schnelle-Kreis, J., Zhang, X., Bendl, J., Khedr, M., Jakobi, G., Schloter-Hai, B., Hovorka, J., and Zimmermann, R.: Integration of air pollution data collected by mobile measurement to derive a preliminary spatiotemporal air pollution profile from two neighboring German-Czech border villages. Sci. Total Environ., 722, 137632, https://doi.org/10.1016/j.scitotenv.2020.137632, 2020a.

Liu, X., Zhang, X., Schnelle-Kreis, J., Jakobi, G., Cao, X., Cyrys, J., ... and Khedr, M.: Spatiotemporal Characteristics and Driving Factors of Black Carbon in Augsburg, Germany: Combination of Mobile Monitoring and Street View Images. Environ. Sci. Technol., https://doi.org/10.1021/acs.est.0c04776, 2020b.

Madueño, L., Kecorius, S., Löndahl, J., Müller, T., Pfeifer, S., Haudek, A., Mardoñez, V., and Wiedensohler, A.: A new method to measure real-world respiratory tract deposition of inhaled ambient black carbon, Environ. Pollut, 248, 295-303, https://doi.org/10.1016/j.envpol.2019.02.021, 2019.

Markowicz, K. M., Ritter, C., Lisok, J., Makuch, P., Stachlewska, I. S., Cappelletti, D., Mazzola, M., and Chilinski, M. T.: Vertical variability of aerosol single-scattering albedo and equivalent black carbon concentration based on in-situ and remote sensing techniques during the iAREA campaigns in Ny-Ålesund, Atmos. Environ, 164, 431-447, https://doi.org/10.1016/j.atmosenv.2017.06.014, 2017.

Masry, E.: Multivariate local polynomial regression for time series: uniform strong consistency and rates, J. Time Ser. Anal., 17, 571-599, https://doi.org/10.1111/j.1467-9892.1996.tb00294.x, 1996.

Pikridas, M., Bezantakos, S., Močnik, G., Keleshis, C., Brechtel, F., Stavroulas, I., Demetriades, G., Antoniou, P., Vouterakos, P., Argyrides, M., Liakakou, E., Drinovec, L., Marinou, E., Amiridis, V., Vrekoussis, M., Mihalopoulos, N., and Sciare, J.: On-flight intercomparison of three miniature aerosol absorption sensors using unmanned aerial systems (UASs), Atmos. Meas. Tech., 12, 6425-6447, https://doi.org/10.5194/amt-12-6425-2019, 2019.

Sadiq, M., Tao, W., Tao, S., and Liu, J.: Air quality and climate responses to anthropogenic black carbon emission changes from East Asia, North America and Europe, Atmos. Environ., 120, 262-276, https://doi.org/10.1016/j.atmosenv.2015.07.001, 2015.

Samad, A., and Vogt, U.: Investigation of urban air quality by performing mobile measurements using a

https://doi.org/10.5194/amt-2020-517
Preprint. Discussion started: 16 February 2021
© Author(s) 2021. CC BY 4.0 License.

Atmospheric Measurement Techniques Discussions

bicycle (MOBAIR), Urban. Climate., 33, 100650, https://doi.org/10.1016/j.uclim.2020.100650, 2020.

Van den Bossche, J., Peters, J., Verwaeren, J., Botteldooren, D., Theunis, J., and De Baets, B.: Mobile monitoring for mapping spatial variation in urban air quality: Development and validation of a methodology based on an extensive dataset. Atmos. Environ., 105, 148-161, https://doi.org/10.1016/j.atmosenv.2015.01.017, 2015.

Van Poppel, M., Peters, J., and Bleux, N.: Methodology for setup and data processing of mobile air quality measurements to assess the spatial variability of concentrations in urban environments. Environ. Pollut., 183, 224-233, https://doi.org/10.1016/j.envpol.2013.02.020, 2013.

Virkkula, A., Mäkelä, T., Hillamo, R., Yli-Tuomi, T., Hirsikko, A., Hämeri, K., and Koponen, I. K.: A simple procedure for correcting loading effects of aethalometer data. J. Air. Waste. Manag. Assoc., 57(10), 1214-1222, https://doi.org/10.3155/1047-3289.57.10.1214, 2007.

Wang, Z., Lu, F., He, H., Lu, Q., Wang, D., Peng, Z.: Fine-scale estimation of carbon monoxide and fine particulate matter concentrations in proximity to a road intersection by using wavelet neural network with genetic algorithm, Atmos. Environ., 104, 264-272, https://doi.org/10.1016/j.atmosenv.2014.12.058, 2015.

Wójcik, M., Sugier, P., and Siebielec, G.: Metal accumulation strategies in plants spontaneously inhabiting Zn-Pb waste deposits, Sci. Total. Environ., 487, 313-322, https://doi.org/10.1016/j.scitotenv.2014.04.024, 2014.

Zhou, H., Lin, J., Shen, Y., Deng, F., Gao, Y., Liu, Y., Dong, H., Zhang, Y., Sun, Q., Fang, J., Tang, S., Wang, Y., Du, Y., Cui, L., Ruan, S., Kong, F., Liu, Z., and Li, T.: Personal black carbon exposure and its determinants among elderly adults in urban China. Environment International, 138, 105607, https://doi.org/10.1016/j.envint.2020.105607, 2020.